

AN UNSTRUCTURED CHARACTERISTICS SCHEME WITH A LINEAR EXPANSION FOR BOTH FLUXES AND CROSS SECTIONS

Simone Santandrea and Pierre Bellier

Commissariat à l'Énergie Atomique
CEN de Saclay DEN/DANS/DM2S/SERMA
simone.santandrea@cea.fr, pierre.bellier@cea.fr

ABSTRACT

Recently we proposed a linear surface scheme for the Method Of Characteristics (MOC) on unstructured meshes. This scheme provided a linear spatial expansion for the flux in arbitrary geometries, based on surface values interpolation. In this paper we present a further development of this method, accepting now the same kind of spatial variation inside each region for the cross sections. This scheme could be used for example in depletion calculations, where fluxes and cross sections should have the same spatial gradients.

Key Words: Method of Characteristics, Higher order methods, Higher order expansion of cross sections

1. INTRODUCTION

Much work has been devoted in recent years to the development of the unstructured characteristics method. [2] Probably the most important limit of the MOC is due to the spatial constant approximation for fluxes and collision sources. Much of the work done to improve the method was devoted in expanding a higher spatial dependence over volume coefficients of the computational mesh. For example Halshall [3] expresses collisions sources in function of three spatial moments, in order to offer a linear variation. In a recent work we have introduced a different scheme that interpolates linearly from average surface and volume values, we have called it Linear Surface (LS) scheme. This scheme has a lower computational complexity with respect to previous approaches, and behaves well for fluxes with strong gradients. [1]

In this work we show a new development related to the LS scheme. The problem we want to address is that of maintaining a coarse geometry adapted to a higher order scheme also in nuclide evolution calculations. Even if cross sections are supposed to be constant inside each computational region at the first step of an evolution calculation, they change accordingly to the flux gradient during evolution. If a higher order method does not allow the same spatial expansion for the cross sections, then dubious spatial homogenizations are mandatory. These procedures are often related to physical approximations and errors that are difficult to forecast, and ask for a necessary qualification phase.

Here we recall the basics of the LS scheme and show that the same interpolation used for the flux (and collision sources) is also possible for cross sections. We will also discuss results on a typical BWR assembly that will show the performance of the method.

2. THE LS SCHEME WITH A LINEAR CROSS SECTION

The LS scheme is based on a linear interpolation between cell boundary values of the collision source. These values are then substituted in the transport integral equation, where an integration is then performed over the values of the sources within each region. For a trajectory t crossing cell i in direction Ω we write:

$$q_t(x, \Omega) = q_t(l, \Omega) \frac{x}{l} + q_t(0, \Omega) \left(1 - \frac{x}{l}\right). \quad (1)$$

In (1) x is a local coordinate over the chord intersected by trajectory t over region i , and x is equal to zero at entering and equal to l at exiting. It is worth noting that expression (1) gives rise to a non consistent numerical approximation, in the sense that the same emission source approximated with two different angles does not have the same value in a given point. We have supposed that this does not prevent good convergence behavior. In order to apply (1) we need to have at our disposal the local values for emission densities. In [1] we have shown that a surface constant approximation can be used as a numerical approximation for the continuous quantities inside (1). A delicate issue is to correctly match the average volume sources that results from using (1) with volume average values that result from the balance equation. This problem can be solved [1] by allowing the source values to be discontinuous at the interfaces between regions. Here we only recall that the final flux representation consists of a surface and a volume component (not independent one with respect to the other).

As in standard MOC, the LS scheme is based on two equations: the transmission and the balance equation. The first equation is obtained by replacing (1) into the analytical transmission equation and this gives:

$$\psi^t(x) = e^{-\tau(0,x)} \psi'_{in,i} + \int_0^x ds e^{-\tau(s,x)} \left[q_{t,i}(l, \Omega) \frac{s}{l} + q_{t,i}(0, \Omega) \left(1 - \frac{s}{l}\right) \right], \quad (2)$$

where the symbol τ is the optical length between the two points inside the parenthesis. The results obtained when using a constant approximation for the cross section inside each computational region are given in [1]. Here we suppose that a similar approximation to (1) also applies to the total cross section that implicitly appears inside τ . Introducing such approximation into (2) gives the following analytical transmission formula:

$$\psi^t(x) = e^{-\tau(0,x)} \psi'_{in,i} + \int_0^x ds e^{-\left[\bar{\sigma} + \frac{\Delta\sigma}{2} \left(1 - \frac{s+x}{l}\right)\right](x-s)} \left[q_{t,i}(l, \Omega) \frac{s}{l} + q_{t,i}(0, \Omega) \left(1 - \frac{s}{l}\right) \right] \quad (3)$$

that can also be written as:

$$\psi^t_{out} = e^{-\tau(0,l)} \psi'_{in} + l \cdot \int_0^1 dx' e^{-\bar{\sigma}l(x'-1) + \frac{l\Delta\sigma}{2}(1-x')x'} \left[q_{t,i}(l, \Omega)x' + q_{t,i}(0, \Omega)(1-x') \right].$$

Developing the exponential inside the integral and retaining only the linear terms gives:

$$\psi_{out}^t = e^{-\bar{\tau}} \psi_{in,i}^t + l \cdot \left[q_0 A_0 + (q_l - q_0 + \frac{q_0 \Delta \tau}{2}) A_1 + \frac{\Delta \tau}{2} (q_l - 2q_0) A_2 - \frac{\Delta \tau}{2} (q_l - q_0) A_3 \right] \quad (3-a)$$

where $\tau_0 = \sigma(0)l$ and $\tau_l = \sigma(l)l$, and $\Delta \tau = \tau_l - \tau_0$, $\sigma(0)$ and $\sigma(l)$ are the values of the total cross section at the entering and exiting side of the region respectively and the transport coefficients A can be computed by the recursive formula:

$$A_{i-1} = \frac{1 - \tau A_i}{i}, \quad i > 0$$

In appendix A it is shown that the linear expansion of the exponential that allows to write (3-a) is a very good approximation of the formula (3). The formula (3a) is used to compute surface average values of the flux moments as:

$$\phi_k^\alpha = \frac{1}{4\pi S_\alpha} \int_\alpha dS \int_{(4\pi)} d\Omega A_k(\Omega) \psi(\mathbf{r}, \Omega) \sim \frac{1}{S_\alpha} \sum_{\substack{\omega_n \in S_N \\ \Gamma \cap S_\alpha}} \omega_n \underbrace{\frac{\omega_\perp(t)}{[\Omega \cdot n]}}_{\delta S^t} A_k(\Omega_n) \psi_\alpha^t(\Omega_n). \quad (3-b)$$

The balance equation is then deduced from the well known integro-differential transport equation:

$$(\Omega \nabla + \sigma) \psi = q$$

integrated in the space-angle domain. As in the standard LS method a duality exists between the average values obtained by conservative equations and average quantities obtained adopting the hypothesis of a linear variation inside each region. One new difficulty is due to the fact that, due to the supposed linear variation of the cross sections, one can directly express only the conservative average total reaction rate in a given region i as:

$$\begin{aligned} \tau_{C,i}^k &= \frac{1}{4\pi V_i} \int_{4\pi} d\Omega A^k(\Omega) \int_{V_i^+(\Omega)} dS_\perp \int ds \sigma(s) \psi(s) = \\ &= \frac{1}{4\pi V_i} \int_{4\pi} d\Omega A^k(\Omega) \int_{V_i^+(\Omega)} dS_\perp \left[\psi^+ - \psi^- + \frac{q^+ - q^-}{2} l \right]. \end{aligned} \quad (4)$$

This quantity has to be compared to the one obtained by making the hypothesis of linear variation inside the region that is:

$$\tau_C^k = \frac{1}{4\pi V_i} \int_{4\pi} d\Omega A^k(\Omega) \int_{V_i^+(\Omega)} dS_\perp \int ds \left[\tau_0^k \left(1 - \frac{s}{l}\right) + \tau_1^k \frac{s}{l} \right] = \sum_{\alpha \in i} \Gamma_\alpha \sigma_\alpha^- \phi_\alpha^-$$

where ϕ_α^- is the moment surface flux per side that is computed in order to preserve the average reaction rates (4), σ_α^- is the inward value of the cross section and coefficients Γ_α describes the geometrical average operator. [1] The quantity ϕ_α^- is explicitly given by:

$$\phi_{\alpha,k}^- = \phi_k^\alpha + C_k^i \quad (5)$$

where the normalization constant is computed as:

$$C_k^i = \frac{\tau_{C,i}^k - \sum_{\alpha \in i} \Gamma_\alpha \Sigma_\alpha^- \phi_\alpha^k}{\Sigma_{t,i}}. \quad (6)$$

Condition (6) only forces the conservation of total reaction rates; the other kinds of reaction rates are not preserved. Moreover the average flux computed by (5) cannot give the good average reaction rate, that is to say:

$$\langle \Sigma_\alpha^- \phi_k^{\alpha,-} \rangle = \tau_C^K \neq \langle \Sigma_\alpha^- \rangle \langle \phi_k^{\alpha,-} \rangle. \quad (7)$$

Equation (7) implies that the conservative reaction rates values cannot be accessed directly from the average fluxes and cross sections.

3. COUPLING GEOMETRIES WITH LINEAR CROSS SECTIONS AND CONSTANT ONES

In an integrated environment such as APOLLO2 [4], each solver has to be able to interact with the data coming from other modules. As for cross sections the usual assumption is the constant representation in each region of a given mesh. In this section we show how we couple geometries where cross sections are supposed to be step-wise constant, with geometries that adopt a linear surface representation for cross sections. Two steps are to be considered. The first one is the interpolation of the step-wise cross sections in the fine mesh geometry to give surface linear cross sections in the coarse mesh geometry. To obtain such interpolation two kind of parameters are necessary, the volume average values and the surface average ones. The second step is to retrieve the constant fluxes in the fine mesh geometry from the coarse one. The first step is quite simple since the volume average values are given by:

$$\bar{\Sigma}_I = \frac{\sum_{i \in I} \Sigma_i V_i}{\sum_i V_i} \quad (8)$$

where the two sums are done over all “micro” regions belonging to “macro” region I, while the surface values are obtained from the neighbouring surface values at each surface, rescaled by a constant correction that is computed to preserve the value in (4):

$$\Sigma_\alpha^- = \Sigma_{t(\alpha,I)} + C_I \quad (9)$$

where $t(\alpha,I)$ is the “micro” region number that share the side α with I , and the constant C is obtained as

$$C_I = \sum_{\alpha \in I} \Gamma_\alpha \Sigma_\alpha - \bar{\Sigma}_I. \quad (10)$$

Formulas (8-10) completely define the interpolated linear cross sections. This allows performing a linear surface calculation with the method described in section 2. The final step consist in retrieving fluxes and reaction rates over the original mesh (where cross section data are supposed to be constant). This can be done by computing the average flux in the fine mesh, supposing the linear variation over the coarse mesh that is given by the computed flux. This assumption leads us to write fine fluxes as:

$$\phi_i = \sum_{\alpha \in I} \Xi_{\alpha,-}^i \phi_{\alpha,-} \quad (11)$$

that shows that we obtain the average flux of each “micro” region contained in I as a linear combination of inward surface fluxes of region I . The coefficients Ξ are given by:

$$\Xi_{\alpha,-}^i = \frac{1}{V_i} \int_{\alpha} dS \int_{(2\pi^+)} d\Omega |\Omega \cdot n| l_i \left(1 - \frac{m}{l_I}\right). \quad (12)$$

where l_i and l_I are the chords lengths that, on a given trajectory starting from a point on surface α on direction Ω , separate this point to, respectively, the middle of the point in region i and the exiting point of region I . The value m is the average of the distance of the exiting and entering points in region i with exiting and entering points in region I .

The microscopic fluxes are the final result that can be directly coupled with other methods.

4. RESULTS AND COMPARAISONS FOR A BWR TEST CASE

In this section we present some comparisons for a rodged BWR assembly. The case we present here is a rodged 8x8 BWR assembly, which we have computed with the two spatial meshes that are shown in figure 1a and 1b. All data and figures of the following computations have been provided by an interface program developed by I. Zmijarevic [5] that generates input data for APOLLO2 calculations. Figure 1a represents the fine mesh geometry, where all cross sections are constant over each region and comprises 362 regions. Figure 1b gives the mesh where cross sections are linearly interpolated and comprises 288 regions. It is important to note that not all regions in this mesh contain linear cross sections: only those regions that results from an agglomeration of heterogeneous cells have interpolated linear cross sections. The fine mesh geometry has been chosen since it is very well converged with respect to mesh refinement. The physics of the problem are characterized by very strong flux heterogeneities because there are four different fuel enrichments plus a gadolinium pin (that is discretized into 11 regions). Moreover, the water density changes between the internal and the external parts of the box (40% of volumetric vapor fraction is present inside the box while the outer part of the box contains single phase water). Finally, the presence of the rod generates a strong flux gradient in the next zone. We have computed this case with a 16 group P0 transport corrected cross sections library that was obtained from an optimized scheme recently developed in APOLLO2. [6]

There are two differences between the two meshes. The first is that fuel pins in the coarse geometry are discretized with only one internal ring that coincides with the innermost ring of the three internal rings used for the fine geometry. Therefore cross sections are linearly interpolated in the fuel pins external regions of the coarse geometry. The second difference concerns the gadolinium pin where only 4 of the initial 11 rings are preserved, and a consequent linear interpolation is done in every internal region.

The local variation in the cross sections is due on one hand to the self shielding process, and on the other hand to the nuclide evolution process. The stronger is this local variation of the cross sections the more difficult will be to do a good interpolation. In order to increase the difficulty we have performed an evolution of 50 steps, until a final burn-up of 60.000 Mwd/t. This strongly enhances the local cross section gradient. Figure 2 shows the absolute error in the integrated fission rate per cell. The maximum relative error is found in the gadolinium pin and it amounts to

0.2%. The computed eigenvalue for the fine mesh case is 0.99597 while for the coarse mesh geometry we obtain 0.99643, while computational times are respectively of 8.17 sec. and 5.77 sec. We have used the standard approach in APOLLO2 for the MOC, which is to accelerate the external iterations by a synthetic operator. [1] In the present context this gives us only 4 external iterations for the standard LS method, with only one internal transport iteration per group and per external iteration, which gives a total of 64 transport sweeps, while we have 3 external iterations and 48 transport sweeps for the new LS method. The difference in computational time is approximately proportional to the number of regions, and this shows that there is not a great over-head due to the new algorithm.

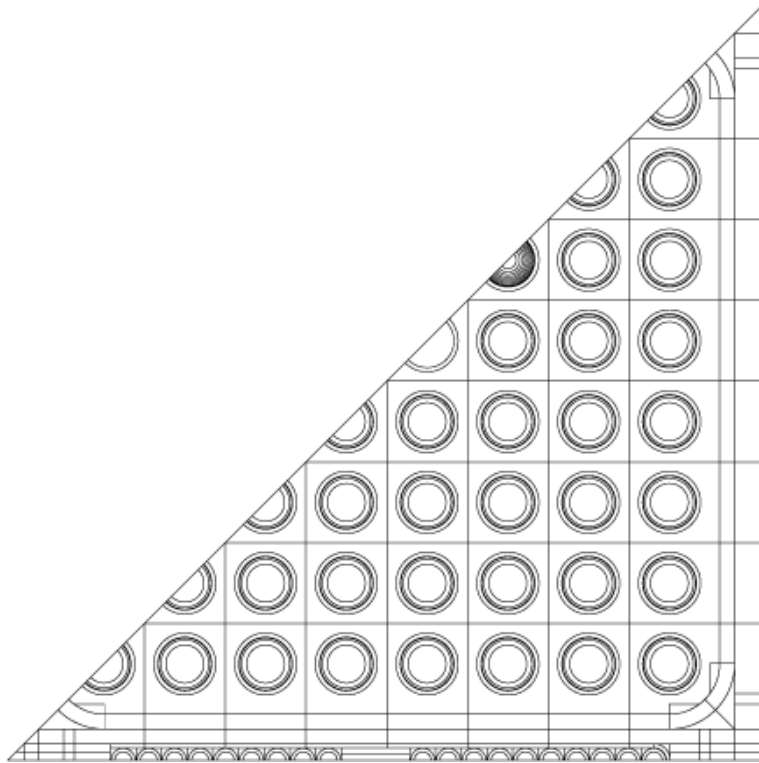


Figure 1a: Computational mesh for constant cross sections.

We have used the LS DP_N synthetic operator [1] computed with constant cross sections even in the case of linear cross sections. This approach has shown to be effective in our (quite severe) case but we do not suppose it to be valid in all configurations. In the next future we will address the item of the necessary modifications to the LS DP_N method to be consistent with the linear cross sections.

5. CONCLUSIONS

In this paper we have considered a numerical scheme that takes into consideration a linear variation of the cross section inside the computational mesh. Our work is done in a framework adapted to the LS MOC, that we have previously developed for the standard case of piece-wise constant cross sections. The numerical representation chosen for the cross sections is therefore coherent with the LS algorithm. The major drawback of the approach is related to a more complicated transmission equation (3-a) that includes the cross section variations along each trajectory. Another main difference with the standard method is the fact that we cannot compute

directly a conservative value of the flux, but only a conservative value of a given reaction rate type. We have arbitrarily chosen to preserve the total reaction rate. All the other reaction rates types are not preserved.

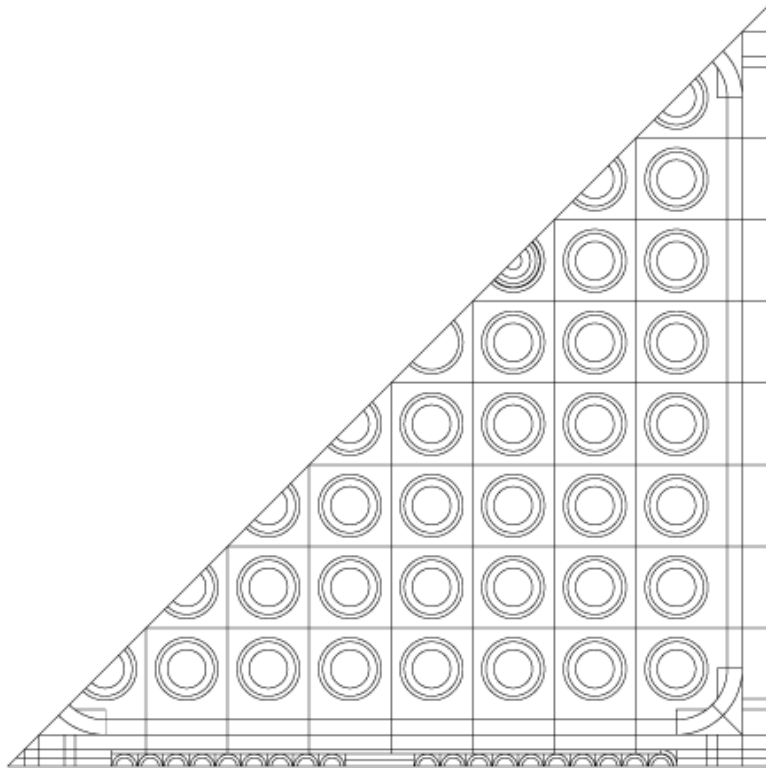


Figure 1b: Computational mesh for linear cross sections.

Our results for a BWR assembly with strong gradients show good accuracy. For this (severe) case the new method can reduce the computational time while preserving accuracy. We will apply this method extensively to PWR and BWR assemblies, and go through a necessary evaluation phase to understand the actual range of our approach.

APPENDIX A: AN ESTIMATION OF THE ERROR INDUCED BY THE TAYLOR EXPANSION IN FORMULA (3a)

To estimate the error related to the Taylor expansion of the exponential in formula (3) one can write the ratio between the first term of this expansion and the first neglected one as follows:

$$\varepsilon_{rel} = \frac{\int_0^1 dx e^{\tau(x-1)} \Delta \tau^2 (1-x)^2 x^2}{3 \frac{1-e^{-\tau}}{\tau}} < \frac{\Delta \tau^2}{3} \int_0^1 dx e^{\tau(x-1)} (1-x)^2 x^2.$$

This gives a correct estimate of the relative error that we make by neglecting the first non-linear term in the Taylor development. By direct integration one finds that:

$$\varepsilon_{rel} < \left(\frac{\Delta\sigma}{\sigma}\right)^2 \frac{1 - e^{-\tau} + \frac{6}{\tau} \left(2 \frac{1 - e^{-\tau}}{\tau} - 1 - e^{-\tau}\right)}{\tau} < 0.03 \left(\frac{\Delta\sigma}{\sigma}\right)^2,$$

which show that the first neglected term is always small. We suppose that higher order terms do not give (even after summation) contributions of a greater order.

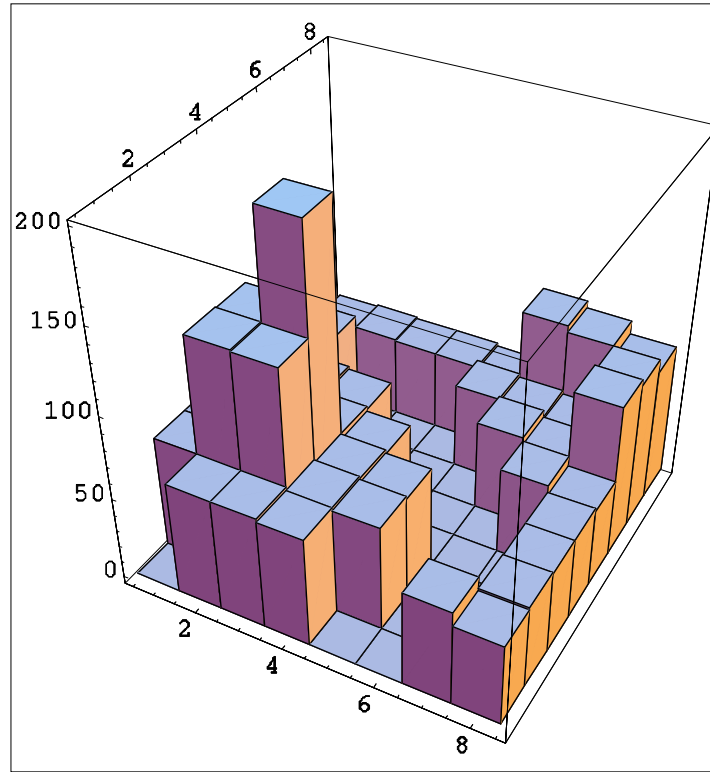


Figure 2: Absolute relative error on the fission rate per cell. The values are in pcm (10E-05). The maximum value is 198pcm in the gadolinium cell

REFERENCES

1. S. Santandrea, “*Linear surface characteristic scheme for the neutron transport equation in unstructured geometries*,” Proceeding of Physor2006, 10-14 Septembre 2006 Vancouver, B.C.
2. Nam Zim Cho, 2005. “*Fundamentals and recent developments of reactor physics methods*”, Nuclear Engineering and Technology, 37, 25-78.
3. Halsall, M.J., 1980. *CACTUS, a Characteristics Solution to the Neutron Transport Equation in Complicated Geometries*. AEEW-R 1291, Atomic Energy Establishment, Winfrith, Dorchester, Dorset, United Kingdom.

4. Sanchez, R., Mondot J., Stankovski, Z., Cossic, A., Zmijarevic, I., 1988. *APOLLO II: A user-oriented, portable, modular code for multigroup transport assembly calculations*. Nuclear Science and Engineering 100, 352-362.
5. Zmijarevic, I. *Personal Communication*
6. Zmijarevic, I, Masiello, E., Sanchez, R. *Flux reconstruction methods for assembly calculations in the code APOLLO2*. Proceeding of Physor2006, 10-14 September 2006 Vancouver, B. C.